Microstructural Examination of Semi-Interpenetrating Networks of Poly(*N*,*N*-dimethylacrylamide) with Cellulose or Chitin Synthesized in Lithium Chloride/*N*,*N*-Dimethylacetamide

Sheila L. Williamson, R. Scott Armentrout, Roger S. Porter,[†,‡] and Charles L. McCormick*

Department of Polymer Science, The University of Southern Mississippi, Hattiesburg, Mississippi 39406-0076

Received May 6, 1998; Revised Manuscript Received September 22, 1998

ABSTRACT: Semi-interpenetrating networks (SIPNs) of poly(*N*,*N*-dimethylacrylamide) (DMAm) containing cellulose or chitin were prepared in 9%LiCl/*N*,*N*-dimethylacetamide (DMAc) as the homogeneous reaction medium. *N*,*N*-Methylenebisacrylamide (MBAm) was utilized as the cross-linking agent with 2,2′-azobisisobutyronitrile (AIBN) as the initiator. The respective SIPNs contained 25, 12, and 6 wt % cellulose or 6 wt % chitin. A control DMAm hydrogel (without polysaccharide) was also synthesized in 9%LiCl/DMAc. The 25 wt % cellulose DMAm SIPN was found to be unique, differing from the other compositions prepared, possessing a 6-fold higher modulus than the DMAm control. The enhancement in mechanical stiffness was attributed to intimate molecular interactions and complexation between cellulose and DMAm. The presence of the extended cellulose chains within the DMAm matrix creates a more open network in the nonsolvated state as reflected in DSC and fluorescence experiments. It is this molecular level interaction of cellulose with DMAm that enhances the physical properties in the first SIPN composite to utilize unmodified cellulose and chitin. In the solvated state, the microdispersed polysaccharide hydrogen bonds with the DMAm matrix increases the rigidity of the network yet allows reversible hydration as reflected in rheology, equilibrium swelling, and fluorescence experiments.

Introduction

During the last fifteen years, our research group[1−8] has been involved in modification reactions involving biopolymers including polysaccharides cellulose and chitin, possessing stiff 1,4-β-D-glc*p* and 1,4-8-D-glcNac*p* repeating sequences. One challenge in attaining uniform reactions with control over the degree of substitution has been to find a suitable solvent for the polysaccharide. In the late 1970s and early 1980s, researchers in our laboratories[3] demonstrated that lithium chloride (LiCl)/*N*,*N*-dimethylacetamide (DMAc) served as a good solvent for cellulose, allowing a variety of uniform reactions to be conducted under homogeneous conditions. An added benefit of this solvent was its utility for conducting spectroscopic investigations and separations of reactants and products. Up to that time, uniform reactions on cellulose were limited due to heterogeneous reaction conditions or the degrading nature of the many solvents.

Subsequent work in our laboratories[7] and at other facilities[9] showed that at high concentrations of cellulose (nearing 15% (w/w) for a weight average molecular weight of 182 000), a biphasic region with nematic texture could be induced by shearing. Utilizing experimentally determined molecular weights and a persistence length of 252 × 10^{-8} cm in LiCl/DMAc,[7] it was estimated from Flory's predictions that a critical concentration of 24% (w/w) cellulose would be required for spontaneous formation of a stable anisotropic phase. A model with chloride ions hydrogen bonded to the cellulose hydroxyl groups and stabilized by DMAc complexed lithium cations was proposed (supported by NMR and viscosity studies) to rationalize the rather long persistence length.[7]

In this research, we investigate the possibility of preparing novel semi-interpenetrating networks (SIPNs) combining two key elements of our previous research with LiCl/DMAc: (a) the ability to conduct facile polymerizations and (b) the maintenance of rodlike structures for cellulose (and chitin) in homogeneous conditions conducive to intimate component mixing. Furthermore, we examine the properties of the resulting networks. Structural characterization of local microstructures utilizing fluorescent labels indicates that the presence of the polysaccharide affects the microenvironments within the continuous DMAm matrix, possibly due to competitive hydrogen bonding in the presence of highly dispersed cellulose chains.

Experimental Section

Materials. Reagent grade cellulose (J. T. Baker), chitin (Sigma), and lithium chloride (Aldrich) were used without purification. *N*,*N*-Dimethylacrylamide (DMAm) was obtained from Aldrich and distilled under vacuum prior to use. *N*,*N*-Methylenebisacrylamide (MBAm) and 2,2′-azobisisobutyronitrile (AIBN) were recrystallized from ethyl acetate and acetone, respectively, twice prior to use. Other reagent grade chemicals were obtained from Aldrich and used as received.

Preparation of *N*-[2-[[[5-(Dimethylamino)-1-naphthyl]-sulfonyl]amino]ethyl]-2-acrylamide (DanEAm). This fluorescent label was synthesized as described in the literature[10] and was chosen so that it would be close to the backbone of the DMAm of the SIPN. This is desirable to investigate the microenvironment of the DMAm network. The amount of label incorporated in the SIPNs was of the order of 10^{-5} mol.

LiCl/DMAc Solvent. Lithium chloride (LiCl) solutions 9% w/w in *N*,*N*-dimethylacetamide (DMAc) were prepared at 100 °C. The solvent was allowed to cool to room temperature before use.

[†] Polymer Science & Engineering Department, University of Massachusetts, Amherst, MA 01003.
[‡] Deceased.

10.1021/ma980718n CCC: $15.00
Published on Web 10/30/1998

Polysaccharide Dissolution. Into a dry, 250 mL, three-necked flask, fitted with nitrogen inlet/outlet and mechanical stirrer, were added 100 mL of 9%LiCl/DMAc and the appropriate amount of preswollen polysaccharide. The cellulose and chitin were preswollen by utilizing a technique reported by McCormick et al.[11] The mixture was stirred at room temperature until dissolution was complete (approximately 1 h for cellulose and 10 h for chitin). The chitin solutions contained some particulate requiring filtration prior to use.

DMAm SIPN Preparation. The DMAm SIPN was formulated in a 100 mL one-necked flask fitted with a septum including inlet/outlet adapters. The polysaccharide solution (1, 2, or 5% w/w cellulose or 0.8% w/w chitin) in 9%LiCl/DMAc (30 mL) was placed in the flask, followed by 4.68 mL (4.54×10^{-2} mol) of DMAm, 0.225 g (1.46×10^{-3} mol) of MBAm, and 0.015 g (9.1×10^{-5} mol) of AIBN. The entire mixture was sparged with nitrogen for approximately 10 min. The mixture was then transferred to test tubes (10 mm i.d.) by syringe (approximately 10 mL in each test tube) and kept closed under a nitrogen purge. The test tubes were then placed in a 60 °C oil bath for 24 h. Subsequently, the samples were removed from the test tubes, cut into circular disks and dialyzed in DMAc for 1 week followed by dialysis in deionized water for an additional week.

DMAm Control Preparation. The same procedure was utilized to synthesize the DMAm control system without the polysaccharide.

Methods. *^{13}C Nuclear Magnetic Resonance (NMR) Spectroscopy.* ^{13}C NMR solid-state spectra were obtained with a Bruker 400 MHz NMR spectrometer utilizing a cross-polarization magic angle spinning (CP/MAS) technique. ^{13}C NMR solution spectra were obtained with a Bruker 300 MHz NMR spectrometer. The deuterated solvent employed for all samples was dimethyl sulfoxide (DMSO-d_6) with tetramethylsilane (TMS) as an additional internal reference.

Rheological Measurements. The storage modulus was determined using a Rheometrics Scientific Dynamic Stress Rheometer SR-200. The experiments were performed at various temperatures with a frequency sweep of 1−100 rad/s and a constant strain of 2% using 25 mm diameter serrated parallel plate geometry. The temperature was controlled with a Polyscience Digital Temperature Controller 9110-RH and held within ±0.05 °C. The samples were measured in the deionized water swollen state. To obtain shear storage moduli that were not influenced by compression, each sample was evaluated at various gap settings such that the modulus versus $(\lambda^{-2} - \lambda)$ was linear, where $\lambda = l/l_o$; l_o and l being the height of the sample before and after the force is applied. The modulus values reported are the extrapolated values corresponding to zero normal force, since it has been shown that normal force is proportional to $(\lambda^{-2} - \lambda)$ by eq 1[12]

$$\frac{F}{A} = G_o(\lambda^{-2} - \lambda) \tag{1}$$

in which F represents the normal force required to compress the sample to length, l, A is the initial cross-sectional area of the sample, and G_o is the equilibrium shear modulus.

Differential Scanning Calorimetry (DSC). DSC analysis was performed with a Mettler TAS811 thermal analyzer equipped with a DSC 305 differential scanning calorimetry cell. Dry samples, 5−10 mg, were prepared in aluminum pans and sealed. A three-cycle method was utilized from 25 to 250 °C at a rate of 10 °C/min with a nitrogen purge. The resulting data were normalized to the original sample weight.

Thermal Gravimetric Analysis (TGA). TGA analysis was conducted with a Mettler TGA850 thermal gravimetric analyzer. Dry samples were directly weighed into aluminum oxide crucibles (10−20 mg). A heating rate of 10 °C/min was maintained from 25 to 600 °C. The resulting TGA traces were normalized to the original sample weight to yield the percent weight loss as a function of temperature.

Equilibrium Swelling. After dialysis of the DMAm control system and the SIPNs, the samples were dried at room temperature for 1 week and then vacuum-dried at 50 °C for 48 h. The individual samples were then allowed to swell for 3 weeks in selected solvents. The equilibrium solvent content (ESC) was calculated from eq 2:

$$\mathrm{ESC} = \frac{\mathrm{wt(SIPN)} - \mathrm{wt(xeroSIPN)}}{\mathrm{wt(xeroSIPN)}} \tag{2}$$

where wt(SIPN) represents the weight of the sample in its solvated state and wt(xeroSIPN) is the weight of the sample in its dried state.[13−15] The equilibrium solvent content was calculated as a mean value of three samples of a given SIPN type. The SIPN systems were evaluated for solvent content in deionized water and in a binary solvent system of acetone and deionized water. The acetone content was varied from 75% (v/v) acetone to 99% (v/v) acetone.

Fluorescence Spectroscopy. UV measurements were conducted with a Hewlett-Packard 8452A diode array spectrophotometer and the fluorescence spectra were measured at 25 °C with an Edinburgh T-Geometry fluorometer. Dried, dansyl labeled DMAm and C5DMAm SIPNs were swollen in different compositions of acetone and deionized water (75% acetone to 99% acetone). The samples were allowed to equilibrate in a 25 °C water bath for 1 week.

The dansyl labels on the respective samples were excited at 330 nm and the steady-state emission spectra were monitored from 350 to 640 nm. Slit widths were varied from 1 to 5 nm, depending on the solvent composition. The resulting spectra were normalized to total fluorescence intensity. The bimodal spectra were deconvoluted by utilizing Peakfit software with a best fit analysis program of four possible functions (Gaussian, Voight, Lorentzian, Pearson).

The Perrin−Weber equation[16] (eq 3) was used to calculate the overall rotational diffusion coefficient, D_r, of the dansyl labels from the steady-state fluorescence anisotropy measurements.

$$r_o/\langle r\rangle = 1 + \tau/\theta = 1 + 6D\tau \tag{3}$$

$\langle r\rangle$ is the average steady-state anisotropy in the region of the maximum emission wavelength (±20 nm), τ is the average fluorescence emission lifetime, and r_o represents the limiting value of $\langle r\rangle$ in a medium where no rotational diffusion occurs and Brownian motion is frozen. The value for r_o has been determined experimentally to be 0.325 for the dansyl chromophore.[17] The methods for obtaining $\langle r\rangle$ and τ have been discussed previously.[18]

Light Microscopy. Polarized light microscopy was performed with a Nikon OPTIPHOTO2-POL polarizing microscope at room temperature. Nondisturbed portions of the SIPN network were placed on precleaned microscope slides and allowed to air-dry.

Results and Discussion

N,*N*-Dimethylacrylamide (DMAm) was selected as the vinyl monomer network component of the SIPNs. DMAm is relatively hydrophilic and polymerizable via conventional free radical techniques. DMAm has structural characteristics similar to *N*,*N*-dimethylacetamide (DMAc) and, therefore, is expected to allow complete solvation of the cellulose or chitin in the presence of lithium chloride. The mechanism of complexation of LiCl/DMAc with cellulose,[19−22] chitin,[23,24] and polyamides[25] has been extensively investigated. It has been suggested that Li^+ complexes with the carbonyl atoms of up to four DMAc molecules to produce a macrocation, leaving the Cl^- free to hydrogen bond with the hydroxyl or amide protons. This competitive hydrogen bond formation serves to disrupt the existing intra- and intermolecular hydrogen bonding, thereby enabling solubilization.[26] The incorporation of DMAm in the monomer feed did not cause precipitation of the polysaccharide. The solutions remained clear, indicating

Table 1. Weight Percentage of SIPN Components in the Dehydrated State

sample	polysaccharide	DMAm	MBAm
DMAm	none	95.2	4.81
C6DMAm	6.0	89.5	4.57
C12DMAm	11.5	84.3	4.29
C25DMAm	25.0	71.4	3.68
CT6DMAm	6.0	89.5	4.54

homogeneous mixing of the monomer within the polysaccharide solution.

The composition of monomer, cross-linker, and initiator in each reaction was kept constant and the weight percent of polysaccharide in the initial 9%LiCl/DMAc solution was varied in order to observe the effect of the polysaccharide incorporation on the physical properties of the resulting materials.

The SIPNs were dialyzed extensively with DMAc and deionized water (1 week in each solvent) to remove any unreacted monomer from the network. All of the polysaccharide-containing SIPNs remained transparent, except for the 12 wt % and 25 wt % cellulose SIPNs, which were slightly opaque, suggesting possible microphase separation or domain formation. The SIPN samples were first dried to constant weight at atmospheric conditions and then subsequently vacuum-dried for 48 h at 50 °C. All samples were transparent in the dehydrated state, including those showing opacity in the hydrated state. The calculated weight percentages of the various components in the resulting dry samples are shown in Table 1.

The sample nomenclature used in Table 1 and throughout this document indicates the type and corresponding weight percentage of polysaccharide (C = cellulose, CT = chitin) in the dehydrated state. Therefore, sample C25DMAm refers to a SIPN composed of 25 wt % cellulose and 75 wt % cross-linked DMAm in the dehydrated state. The C25DMAm sample has a large weight percent of polysaccharide as compared to the other systems. It should be noted that the 25 wt % composition of cellulose represents the viscosity limit of cellulose for SIPN preparation.

^{13}C NMR Solid State Spectroscopy. Solid state ^{13}C NMR spectra of the DMAm control gel, CT6DMAm SIPN, and C25DMAm SIPN are shown in Figure 1. The presence of the polysaccharide is apparent in both SIPN spectra in the region of 50−100 ppm. The peak pattern for cellulose in the C25DMAm SIPN is identical to that of cellulose alone.

Rheological Experiments. The water-swollen SIPNs containing various weight percentages of cellulose exhibited major differences in mechanical properties during isolation. Therefore, the storage moduli of the DMAm control and the cellulose-containing DMAm SIPN systems were measured. Figure 2 illustrates the ratio of the storage modulus of the cellulose SIPNs to that of the DMAm control gel as a function of the volume fraction of cellulose and temperature. A volume fraction of 1.5 cellulose results in a modulus 6-fold higher than that observed for the unfilled DMAm control gel. This was attributed to a volume fraction effect and/or molecular interaction between the network and polysaccharide.

In 9%LiCl/DMAc, the persistence length of cellulose was found to be 252×10^{-8} cm,[16] which is larger than that reported for cellulose in any other solution. In these SIPN composites, cellulose acts as a fully extended, rigid rod polymer, which also has the capability

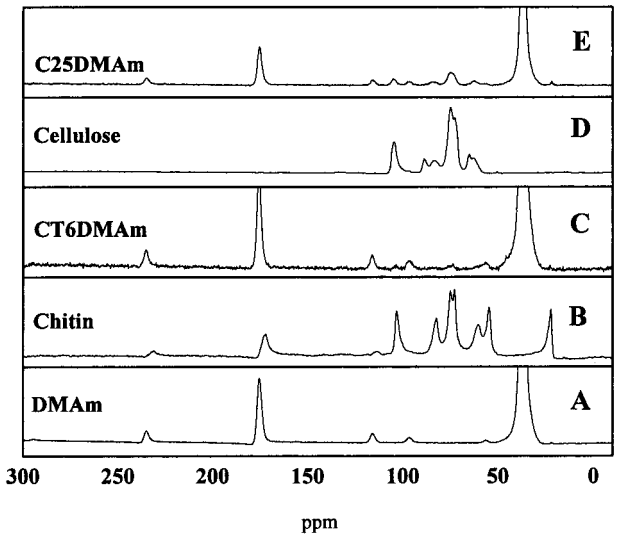

Figure 1. Solid-state ^{13}C NMR spectra of (A) DMAm control gel, (B) chitin, (C) CT6DMAm SIPN, (D) cellulose, and (E) C25DMAm.

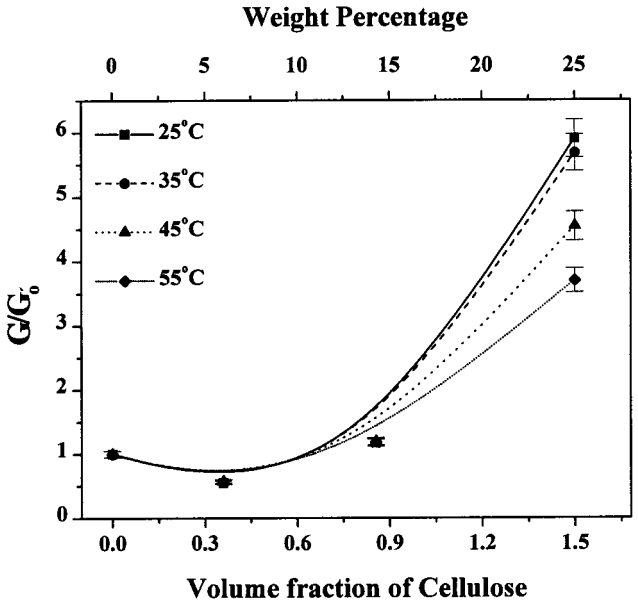

Figure 2. Ratio of storage modulus of the cellulose SIPNs to the storage modulus of the DMAm control gel (in the hydrated state) as a function of the volume fraction of cellulose and temperature.

to hydrogen bond with other cellulose polymer chains as well as the DMAm matrix, explaining the enhancement of physical properties that are observed. The ratio of storage moduli shown in Figure 2 decreases as the temperature increases, suggesting the breakdown of intermolecular interactions that give this material its enhanced mechanical properties at room temperature. It is also apparent that a minimum concentration of cellulose is required for appropriate morphology to develop in order to stiffen the SIPN matrix.

^{13}C NMR Solution Spectroscopy. In an effort to investigate the nature of molecular interactions within the SIPNs, ^{13}C NMR spectra of the various components of the reaction mixture (prior to polymerization) were compared. Figure 3 presents the ^{13}C NMR spectra of (A) 9%LiCl/DMAc solvent, (B) DMAm monomer, (C) 9%LiCl/DMAm, (D) a 1:1 mixture of 9%LiCl/DMAc and DMAm, and (E) a 1:1 mixture of 5 wt % cellulose in 9%LiCl/DMAc and DMAm monomer.

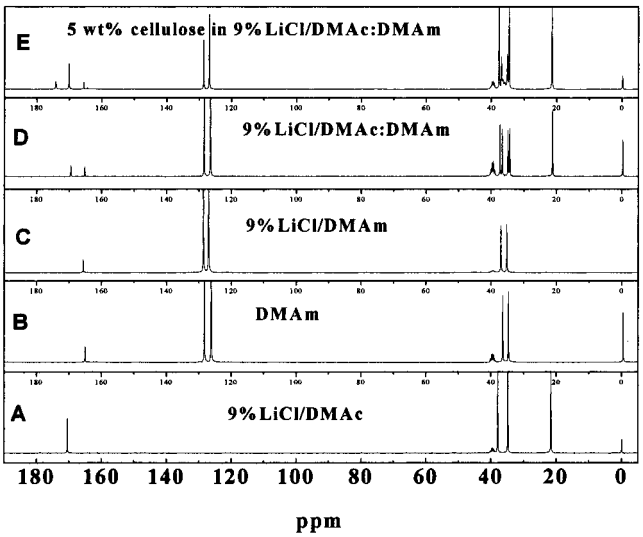

Figure 3. ^{13}C NMR spectra of (A) 9%LiCl/DMAc, (B) DMAm, (C) 9%LiCl/DMAm, (D) 9%LiCl/DMAc:DMAm, and (E) 5 wt % cellulose in 9%LiCl/DMAc:DMAm.

Table 2. Differential Scanning Calorimetry Spectra of Cellulose, DMAm Control, and SIPNs (Second Run)

sample	T_g (°C)	sample	T_g (°C)
DMAm	142	C25DMAm	132
C6DMAm	139	CT6DMAm	138
C12DMAm	136		

It is important to note that the concentrations of the DMAm monomer in this study are much higher than the concentrations utilized for the SIPN formulations. The cellulose resonances do not appear in the spectrum of Figure 3E due to the relatively low concentration, but the effect of the cellulose on the solvent and monomer can be seen in the spectrum. The appearance of an additional carbonyl peak at 174 ppm in Figure 3E is attributed to the shift of a percentage of the DMAm carbonyls to 174 ppm from their original position at 164 ppm. This conclusion is supported by comparing the relative intensities of the peaks in the 1:1 mixture of 9%LiCl/DMAc:DMAm (3D) with those in the 1:1 mixture of 5 wt % cellulose in 9%LiCl/DMAc:DMAm (3E). This shift does not occur in the mixture of DMAm and the solvent, 9%LiCl/DMAc. A similar complexation occurring between cellulose and the DMAm carbonyl may serve to enhance the physical properties of the resulting SIPN composite material after network formation. This proposal will be addressed in the sections to follow.

Differential Scanning Calorimetry. DSC was utilized to examine the transitions as affected by addition of the polysaccharide. The unmodified cellulose control shows no endothermic transition within the temperature range of the experiment. The DMAm control sample displayed one noticeable endothermic transition (T_g) with an inflection point at 135 °C (Table 2). The presence of the polysaccharide does not seem to greatly affect the temperature of this endothermic transition. The transition does broaden and the slope decreases with an increase in polysaccharide concentration. The presence of only one transition implies a high degree of miscibility and a high degree of intermolecular interactions between two components of a SIPN.[27]

Thermal Gravimetric Analysis. To investigate the degree of intermolecular interaction within the SIPNs, degradation properties were investigated as a function of weight percent and type of polysaccharide. The

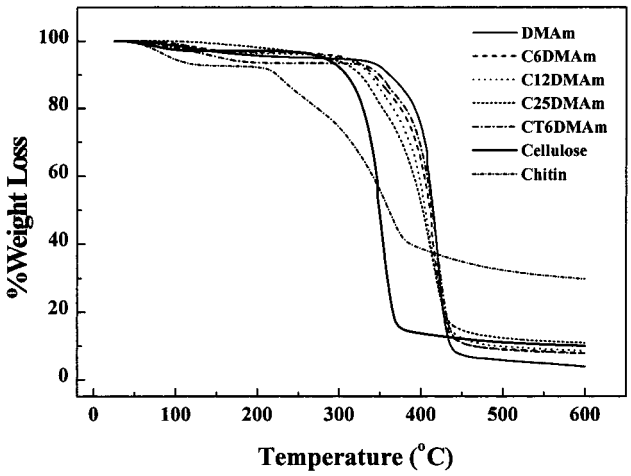

Figure 4. Thermogravimetric analysis profiles for cellulose, DMAm control, and SIPNs.

Table 3. Equilibrium Water Content for SIPNs of (6, 12, and 25 wt %) Cellulose, 6 wt % Chitin, and the Corresponding Control Network in Deionized Water

sample	EWC	sample	EWC
DMAm	20.4 ± 0.6	C25DMAm	16.7 ± 0.6
C6DMAm	16.8 ± 0.7	CT6DMAm	15.3 ± 0.7
C12DMAm	13.4 ± 0.5		

degradation of DMAm SIPNs occurs in one stage over a temperature range between DMAm and polysaccharide controls (Figure 4). This suggests good intermolecular interaction between the DMAm matrix and the linear polysaccharide. If there were no intermolecular interaction, the resulting degradation profile would be expected to occur in two stages, the first occurring at 300 or 350 °C depending on the polysaccharide and the second stage occurring at 400 °C corresponding to the DMAm control system. A control experiment was conducted by combining 25 wt % cellulose with 75 wt % DMAm control matrix and a two stage degradation profile was observed.

Equilibrium Swelling and Microphase Behavior. To further investigate the enhancement of physical properties of the SIPNs, swelling experiments were conducted in deionized water. Table 3 illustrates the average of the equilibrium water content (EWC) determined for each SIPN. The control DMAm gel has the highest EWC, while the C12DMAm SIPN has the lowest EWC. The C25DMAm SIPN has a significantly larger EWC than might be predicted on the basis of increasing content of the less hydrophilic cellulose. However, the 25 wt % cellulose (C25DMAm) SIPN appears to possess both mechanical properties and swelling behavior indicative of an optimized morphology (this will be detailed in a later section).

The volume phase transition has been studied for cross-linked polyacrylamide hydrogels in acetone:water binary solvent systems.[28] This transition is characterized by a decrease in swelling as the acetone concentration is increased. With this literature precedence in mind, a binary solvent swelling experiment was conducted on the SIPN containing 25 wt % cellulose (C25DMAm) and the control gel (DMAm) by utilizing acetone/deionized water ratios of 75:25 to 99:1% (v/v) to determine the effect cellulose incorporation has on the swelling response of the system.

Figure 5 shows the equilibrium solvent content (ESC) for DMAm and C25DMAm as a function of percent

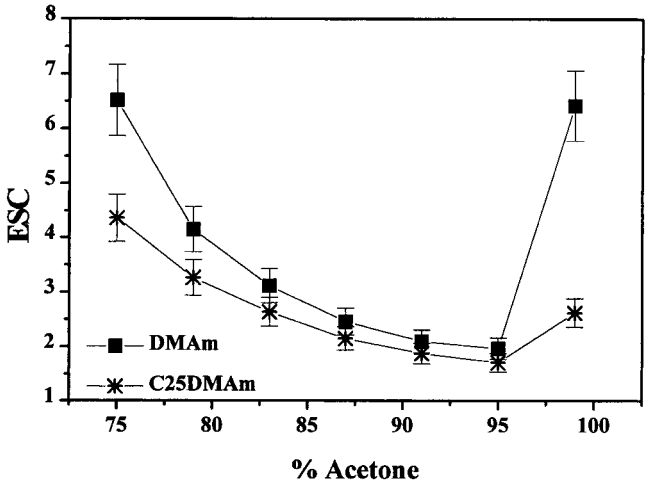

Figure 5. Equilibrium solvent content of DMAm and C25DMAm as a function of solvent composition.

acetone. The DMAm system exhibits a larger initial ESC than the C25DMAm system. However, the DMAm ESC values decrease to those similar to the C25DMAm system as the percent acetone increases to 95%. Above 95% acetone, the DMAm ESC value increases rapidly compared to C25DMAm. Above 95% acetone, network expansion is retarded substantially by the cellulose network element compared to the DMAm control.

Fluorescence Spectroscopy. To gain an understanding of the forces governing the solvation of the polymer networks on a molecular level, DMAm and C25DMAm systems were labeled with a short chain dansyl monomer, (*N*-[2-[[[5-(dimethylamino)-1-naphthalenyl]sulfonyl]amino]ethyl]-2-acrylamide) (DanEAm). The dansyl group is a sensitive fluorescent moiety that has been utilized to investigate polarity and mobility within its microenvironment.[29−35] The change in the fluorescence emission of the dansyl label is due to the formation of a twisted intramolecular charge transfer (TICT) state induced by changes in free volume and/or micropolarity surrounding the label. Upon the formation of the TICT state in a polar or nonrigid microenvironment, the maximum fluorescence emission is centered at ∼580 nm.[29,30] However, in a nonpolar or highly viscous microenvironment, the label assumes a coplanar conformation characterized by a maximum in fluorescence emission at ∼430 nm and an increase in fluorescence quantum yield. Whereas steady-state fluorescence measurements may be utilized to determine qualitative information concerning the polarity and viscosity of the microenvironment around the dansyl label, it is difficult to discern which property (polarity or microviscosity) most affects the fluorescence emission. Therefore, to distinguish between polarity and viscosity effects, steady-state fluorescence depolarization studies have been utilized to determine the rotational diffusion coefficient of the chromophore as a function of solvent composition for the C25DMAm SIPN and the control DMAm. The rotational diffusion coefficient of the dansyl chromophore is related to the microviscosity within the polymeric network and, therefore, reflects the rigidity of the polymeric network on a molecular level.

Steady-State Fluorescence. Figures 6 and 7 illustrate the normalized steady-state emission spectra of the DMAm control system and C25DMAm SIPN as a function of solvent composition. The primary feature of these systems is that two emission states are observed

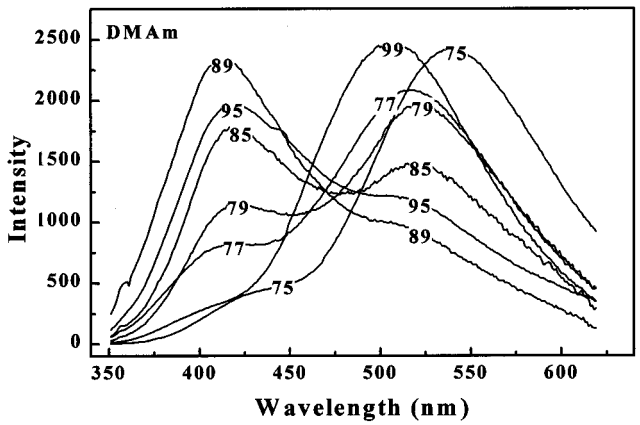

Figure 6. Steady state fluorescence spectra of the DMAm control as a function of solvent composition. The number represents the percent acetone.

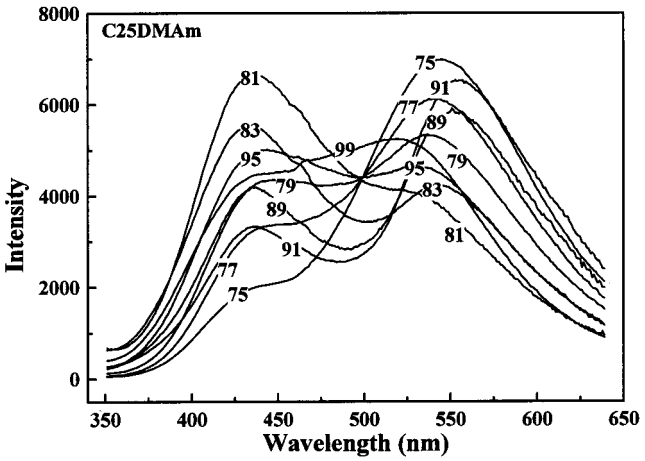

Figure 7. Steady state fluorescence spectra of the C25DMAm SIPN as a function of solvent composition. The number represents the percent acetone.

corresponding to a polar microenvironment (TICT state at ∼525 nm) and a nonpolar/rigid microenvironment (coplanar conformation at ∼425 nm), respectively. These two emission states present within one polymer system have been reported previously in the literature for dansyl-labeled polymer systems.[33,36] Horie and coworkers[33] found one broad emission peak with shoulder development of the polar emission state in dansyl-labeled poly(acrylamide) hydrogels in acetone/water (9/11) at a pH of 3.3. Aiding greatly in this analysis, however, is the fact that the two emission states shown in Figures 6 and 7 for the DMAm control system and the C25DMAm SIPN are more distinct and bimodal than those described in the literature.[33,36]

A control study was performed with the model compound, dansyl-DL-α-aminocaprylic acid cyclohexylamine salt, in the same solvent compositions, and only one emission state was observed with a maximum emission wavelength at ∼520 nm (data not shown) representing the more polar, lower microviscosity, TICT state. Therefore, the development of the bimodal distribution in the dansyl-labeled DMAm control system and C25DMAm SIPN is not a result of the association of the solvent with the label but is rather due to the label partitioning into two distinct microdomains in water:acetone cosolvent mixtures.

The spectra in Figure 6 exhibit fluorescence emission maxima corresponding to the polar/flexible and nonpo-

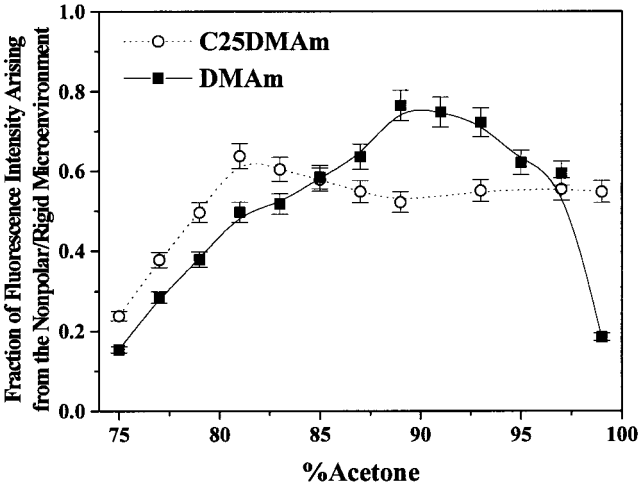

Figure 8. Normalized fraction of fluorescence intensity arising from the nonpolar/rigid microenvironment (coplanar, non-TICT state) for the dansyl-labeled C25DMAm and DMAm systems. (λ_{ex} = 330 nm).

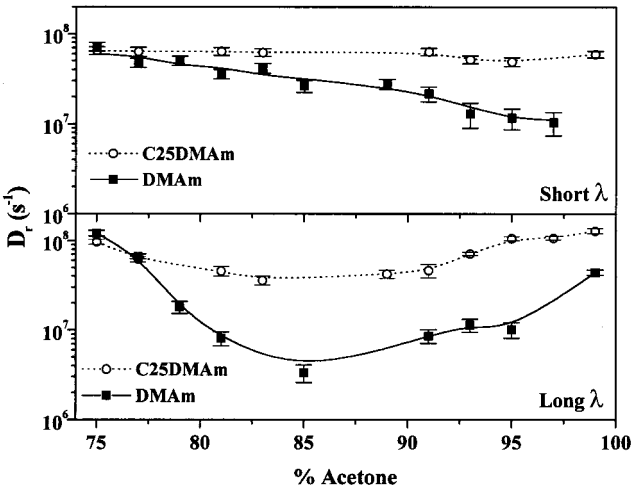

Figure 9. Rotational diffusion coefficients for the dansyl label in the coplanar conformation (short λ_{em}) and the TICT state (long λ_{em}) as a function of solvent composition for the DMAm control and the C25DMAm SIPN.

lar/rigid microenvironments centered around 520 and 420 nm, respectively for the DMAm control. However, in the C25DMAm SIPN system, fluorescence emission peaks are red-shifted to 540 and 430 nm, respectively (Figure 7), indicating that the fluorescent labels are experiencing a more polar, relaxed microenvironment.

The fluorescence emission spectra were deconvoluted and the areas of the two emission peaks were determined. The normalized fraction of fluorescence intensity arising from the dansyl labels that assume a coplanar conformation are shown in Figure 8 as a function of acetone concentration for the DMAm control system and the C25DMAm SIPN. It is important to point out that the fraction of fluorescence intensity arising from the coplanar conformation is not precisely equivalent to the percentage of chromophores present within the nonpolar, rigid microenvironment since the fluorescence quantum yields for the coplanar and TICT states are not equivalent. However, this analysis may be utilized to obtain an estimate of the relative number of chromophores within a given microenvironment.

When the polymer networks are well solvated (low acetone concentrations as shown in Figure 5), the fraction of fluorescence intensity arising from the coplanar conformation is small, indicating that most of the chromophores are located within a polar, flexible microenvironment. However, as the polymer network undergoes a macroscopic collapse, the fraction of fluorescence intensity arising from the coplanar conformation increases since a larger percentage of chromophores are now present in a nonpolar, rigid microenvironment.

Interestingly, at low acetone concentrations (<85%), the fraction of fluorescence arising from the coplanar conformation is higher for the cellulose containing material than for the control, indicating that a larger percentage of the dansyl labels within the SIPN are experiencing a more nonpolar, rigid microenvironment than in the control network. A reasonable hypothesis is that the additional hydrogen bonds between the cellulose hydroxyl moieties and the DMAm mers are responsible for this behavior.

It has been shown by Morawetz that the dansyl fluorescence emission is blue shifted and increases in intensity upon the formation of hydrogen bonds between poly(acrylic acid) and poly(oxyethylene).[37,38] In our case, hydrogen bonding between the rigid-rod cellulose and the DMAm polymer network, as suggested through solution ^{13}C NMR of the monomeric components, could result in nonpolar, rigid microdomains that would lead to the enhancement of the fluorescence emission from the coplanar state, as is shown in Figure 8. These hydrogen bonds effectively increase the network density of the polymer network in the swollen state, therefore enhancing the physical properties of the materials, consistent with data in Figure 2.

As the acetone concentration is increased above 81%, the fluorescence intensity arising from the coplanar conformation levels off for the C25DMAm SIPN but continues to increase for the control material until a maximum is realized at ~89% acetone. The DMAm control undergoes a further collapse leading to an enhancement of the fluorescence emission arising from the coplanar conformation of the dansyl label. However, for the C25DMAm SIPN, the network does not undergo as large a collapse as is seen in the control material. The rigid rod cellulose cross-links act to restrict the collapse of the polymer network, and therefore, a plateau for the fraction of fluorescence arising from the nonpolar microenvironment is realized (Figure 8).

Finally, as the acetone concentration is increased above 89%, the control material experiences a transition to a more polar, flexible structure, as evidenced by a reduction of fluorescence intensity arising from the coplanar conformation. Once again the more polar structure is expected due to the increase in swelling at high acetone concentrations, as is shown in Figure 5.

Steady-State Fluorescence Depolarization. Steady-state fluorescence depolarization experiments measure the mobility of the dansyl label within the polymeric network. By monitoring the steady-state fluorescence anisotropy, r, and the average fluorescence lifetime, τ, the rotational diffusion coefficient, D_r, may be determined. Higher values for the rotational diffusion coefficient indicate greater mobility for the dansyl label. Since the chromophore is covalently bound to the polymeric network by a short spacer, the rotational diffusion coefficient is directly proportional to the segmental mobility of the polymer backbone.[18]

Figure 9 illustrates the rotational diffusion coefficients of the dansyl label assuming the coplanar

Figure 10. Light microscopy photo of dry C25DMAm SIPN film (200×). Figure reduced to 75% for publication.

conformation (short λ_{em}) and TICT state (long λ_{em}) in the DMAm control system and the C25DMAm SIPN as a function of solvent composition. As may be seen in the figure, the rotational diffusion coefficient arising from the coplanar conformation (short λ_{em}) for the DMAm control system decreases linearly as the acetone concentration is increased. This indicates that the label is located in an increasingly nonpolar/rigid microenvironment as the acetone concentration increases (up to 95%). This occurs over the same range as macroscopic network collapse (Figure 5). By contrast, the rotational diffusion coefficient of the dansyl label within the nonpolar/rigid microdomain (short λ_{em}) of the C25DMAm SIPN remains constant with increasing acetone concentrations. This indicates that the conformation of the polymer network within the nonpolar/rigid microdomains cannot undergo further collapse when cellulose is present within the system.

The rotational diffusion coefficient arising from the dansyl labels in the TICT state (long λ_{em}) initially decreases for both systems as the acetone concentration increases, indicating that the dansyl labels within the polar/flexible microdomains begin to experience a more rigid microenvironment. However, the ability of the SIPN network to maintain "open" solvated spaces (enhanced mobility) for a portion of the dansyl label at increasingly high acetone concentrations is remarkable. Incorporation of the rigid-rod cellulose acts as physical cross-links that retard the collapse of the polymer network, leading to the retention of an open conformation.

When the acetone concentration exceeds 90%, the rotational diffusion coefficients of the chromophores increase for the control and SIPN polymer systems, indicating a transition to a more relaxed conformation. However, the magnitude of this transition is much larger for the control material than for the cellulose containing network. This transition to a more relaxed conformation is realized on a macroscopic scale by a reswelling of the three-dimensional network.

It is interesting to observe that the shapes of the curves representing both the composite and the control materials are the same for the nonpolar/rigid and polar/flexible microdomains. However, the magnitudes of the rotational diffusion coefficients for the C25DMAm SIPN are quite different. For acetone concentrations less than 79% (where the polymer network assumes an expanded conformation), the steady-state diffusion coefficients for the dansyl labels within the C25DMAm are less than in the control. This indicates that the rigidity of the polymeric network is enhanced due to the presence of the polysaccharide likely due to the formation of physical cross-links within the DMAm polymer network. However, as the acetone concentration is increased, the steady-state diffusion coefficients for the dansyl labels within C25DMAm are greater than for the control, indicating more flexibility in the composite due to the prevention of complete collapse of the network provided by the presence of the polysaccharide.

Light Microscopy. If hydrogen bonding between the cellulose and DMAm matrix is sufficient in the C25DMAm SIPN, there exists the possibility of the development of macroscopic crystalline order. If long

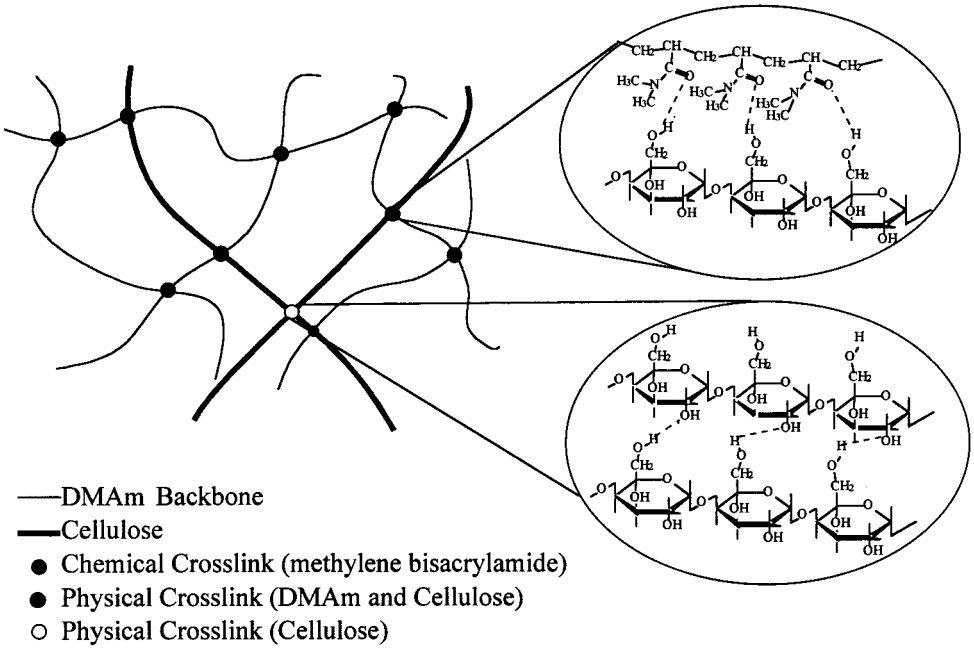

Figure 11. Schematic representation of hydrogen bonding between the DMAm matrix and cellulose that leads to the enhancement of physical properties.

range order is present within the sample, birefringence should be present when the polymer is analyzed under polarized light microscopy. A photograph of a dry C25DMAm SIPN film observed with the light microscope is shown in Figure 10. It is clearly seen that macroscopic crystalline order is evident throughout the sample.

The preparation of the SIPNs was conducted under conditions in which no lyotropic mesophase was present. In other words, the concentration of cellulose (5 wt % in 9%LiCl/DMAc) and DMAm was insufficient to produce orderd cellulose arrays. After the SIPNs were purified to remove residual DMAm monomer, DMAc, and LiCl, the samples were reswollen in deionized water. Polarized light microscopy was used to follow deswelling as water was removed from the SIPN. The birefringence was only observed in the dehydrated state and is reversible when water is introduced to the dehydrated sample. This suggests that there exists an equilibrium of hydrogen bonding between the water and the cellulose containing SIPN. The observed development of microcrystalline order (and the enhanced properties) is a consequence of the rigidity of the extended cellulose chains and their proximity to the polymerizing DMAm during synthesis (Figure 11). The persistence length of 252 Å LiCl/DMAc allows intimate contact for extensive hydrogen bonding with cellulose. The cellulose microdomains are reversible and are easily observed on deswelling the SIPN network.

It is pertinent to note that phase separation of the cellulose within the DMAm matrix does not occur. This continuous matrix of the dehydrated sample is confirmed by the existence of a single T_g and a one-stage thermal degradation profile. The extended cellulose acts to increase the volume within the network, as determined by fluorescence experiments.

Conclusions

Novel semi-interpenetrating networks of cellulose (or chitin) and *N*,*N*-dimethylacrylamide were prepared by utilizing a 9%LiCl/*N*,*N*-dimethylacetamide solvent system. The resulting composites are optically transparent and exhibit a one-stage thermal degradation profile. The C25DMAm SIPN has a 6-fold higher storage modulus and lower equilibrium water content than the DMAm control system.

Steady state fluorescence and fluorescence depolarization experiments of dansyl-labeled DMAm and C25DMAm systems in the expanded state indicate that the presence of cellulose enhances the development of a nonpolar, rigid microenvironment within the polymeric network. The presence of the rigid polysaccharide apparently hinders the complete collapse of the polymer network when placed in a nonsolvent or upon the removal of water, as demonstrated by fluorescence depolarization and DSC measurements. Light microscopy of the C25DMAm SIPN indicates network formation and order development within the system in the dried state. Order is also likely maintained at the molecular level in the hydrated state and is attributed to the formation of hydrogen bonds between the cellulose hydroxyl moieties

Acknowledgment. Support from the Office of Naval Research is gratefully acknowledged. The authors would like to thank Dr. Yuxin Hu for his helpful discussions and Dr. William Jarrett for performing the solid state ^{13}C NMR analysis.

References and Notes

(1) McCormick, C. L.; Lichatowich, D. K. *J. Polym. Sci.: Polym. Lett.* **1979**, *17*, 478−484.
(2) McCormick, C. L.; Lichatowich, D. K.; Pelezo, J. A.; Anderson, K. W. In *Modifications of Polymers*; Carraher, C. E., Ed.; ACS Symposium Series; American Chemical Society: Washington, DC, 1980; No. 121, pp 371−380.
(3) McCormick, C. L. U.S. Patent 4,278,790 1981; application date 1979.
(4) McCormick, C. L.; Callais, P. A. *Polymer* **1987**, *28*, 2317−2323.
(5) McCormick, C. L.; Dawsey, T. *J. Macromol. Sci., Rev. Macromol. Chem. Phys.* **1990**, *C30* (3&4), 405−440.
(6) McCormick, C. L.; Dawsey, T. *Macromolecules* **1990**, *23* (15), 3606−3610.
(7) McCormick, C. L.; Callais, P. A.; Hutchinson, B. H., Jr. *Macromolecules* **1985**, *18*, 2394.
(8) McCormick, C. L.; Shen, T. In *Macromolecular Solutions*; Seymour, R. B., Stahl, G. S., Eds.; Pergamon Press: New York, 1982; pp 101−107.
(9) Chanzy, H.; Peguy, A. *J. Polym. Sci., Polym. Phys. Ed.* **1980**, *18*, 1137.
(10) Shea, K. J.; Stoddard, G. J.; Shavelle, D. M.; Wakui, F.; Choate, R. M. *Macromolecules* **1990**, *23*, 233.
(11) McCormick, C. L.; Dawsey, T. *Macromolecules* **1990**, *23* (15), 3606−3610.
(12) Ilavsky, M.; Bouchal, K.; Hrouz, J. *Polym. Bull.* **1990**, *24*, 619−625.
(13) Mukae, K.; Bae, Y. H.; Okano, T.; Kim, S. W. *Polymer* **1990**, *22*, 206.
(14) Kabra, B. G.; Akhtar, M. K.; Gehrke, S. H. *Polymer* **1992**, *23*, 990.
(15) Yu, H.; Granger, D. W. *Macromolecules* **1994**, *27*, 4554.
(16) Weber, G. *Biochem. J.* **1952**, *51*, 145−155.
(17) Hu, Y.; Horie, K.; Ushiki, H. *Macromolecules* **1986**, *19*, 2253.
(18) Hu, Y.; Armentrout, R. S.; McCormick, C. L. *Macromolecules* **1997**, *30*, 3538.
(19) McCormick, C. L.; Callais, P. A.; Hutchinson, B. H., Jr. *Macromolecules* **1985**, *18*, 2394.
(20) McCormick, C. L.; Shen, T. In *Macromolecular Solutions*; Seymour, R. B., Stahl, G. S., Eds.; Pergamon Press: New York, 1982; pp 101−107.
(21) El Kafrawy, A. *J. Appl. Polym. Sci.* **1982**, *27*, 2435−2443.
(22) El Kafrawy, A. *Chem. Abstr.* **1984**, *100*, 141033h.
(23) Terbojevich, M.; Carraro, C.; Cosani, A. *Carbohydr. Res.* **1988**, *180*, 73−86.
(24) Vincendon, M. *Makromol. Chem.* **1985**, *186*, 1787−1795.
(25) Panar, M.; Beste, L. F. *Macromolecules* **1977**, *10*, 1401.
(26) McCormick, C. L.; Dawsey, T. R. *J. Macromol. Sci., Rev. Macromol. Chem. Phys.* **1990**, *C30* (3&4), 405−440.
(27) Visscher, K. B.; Manners, I.; Allcock, H. R. *Synthesis and Characterization of Poly(organophosphazene) Interpenetrating Polymer Networks*; Interpenetrating Networks; American Chemical Society: Washington, DC, 1994; p 169.
(28) Tanaka, T. *Phys. Rev. Lett.* **1978**, *40*, 821.
(29) Weber, G. *Biochem. J.* **1952**, *51*, 155.
(30) Strauss, U. P.; Vesnaver, G. J. *J. Phys. Chem.* **1975**, *79*, 1558−2426.
(31) Kosower, E. M.; Dodiuk, H.; Tazutake, K.; Ottolenghi, M.; Orbach, N. *J. Am. Chem. Soc.* **1975**, *97*, 2167.
(32) Li, Y. H.; Chan, L. M.; Tyer, L.; Moody, R. T.; Himel, C. M.; Hercules, D. M. *J. Am. Chem. Soc.* **1975**, *97*, 3118.
(33) Hu, Y.; Horie, K.; Ushiki, H. *Macromolecules* **1992**, *25*, 6040.
(34) Horie, K.; Mita, I.; Kawabata, J.; Nakahama, S.; Hirao, A.; Yamazaki, N. *Polym. J.* **1980**, *12*, 319.
(35) (a) Seo, T.; Take, S.; Miwa, K.; Hamada, K.; Iijima, T. *Macromolecules* **1991**, *24*, 4255. (b) Seo, T.; Take, S.; Akimoto, T.; Hamada, K.; Iijima, T. *Macromolecules* **1991**, *24*, 4801.
(36) Leezenberg, P. B.; Frank, C. W. *Chem. Mater.* **1995**, *7*, 1784−1792.
(37) Chen, H.-L.; Morawetz, H. *Eur. Polym. J.* **1983**, *19*, 923.
(38) Bednar, B.; Li, Z.; Huang, Y.; Chang, L.-C. P.; Morawetz, H. *Macromolecules* **1985**, *18*, 1829.

MA980718N